Detection of Huanglongbing Disease in Citrus Using Fluorescence Spectroscopy

S. Sankaran, R. Ehsani

Abstract. *Huanglongbing (HLB) is an important citrus disease greatly affecting the citrus industry in Florida and other parts of the world. Early disease detection would control the spread of this disease through the application of suitable management measures. This study evaluates the application of fluorescence sensing for HLB detection of citrus leaves. A commercial handheld fluorescence sensor was used to collect yellow, red, and far-red fluorescence at ultraviolet (UV), blue, green, and red excitations from healthy, nutrient-deficient, and HLB-infected leaves of two different sweet orange cultivars, Hamlin and Valencia. Evaluation of the fluorescence sensing was performed under laboratory (controlled) and field conditions. The Naïve-Bayes and the bagged decision tree classifiers were trained and tested to assess their performance in classifying the healthy and stressed (nutrient-deficient) leaves. Results revealed that the Naïve-Bayes classifier yielded high classification accuracy under laboratory conditions (higher than 85%), while the bagged decision tree classifier yielded high overall classification accuracy under both laboratory and field conditions (higher than 94%). The bagged decision tree classifier performed better than the Naïve-Bayes classifier, resulting in higher classification accuracy, although the computation time was at least 10 times greater than that of the Naïve-Bayes classifier. In addition, feature extraction using forward feature selection indicated that fluorescence features such as yellow fluorescence (UV excitation) and simple fluorescence ratio (green excitation) contributed toward differentiating healthy leaves from nutrient-deficient and HLB-infected leaves.*

Keywords. *Bagged decision tree classifier, Citrus leaves, Fluorescence sensing, Huanglongbing, Naïve-Bayes classifier.*

Huanglongbing (HLB) or citrus greening is a devastating citrus disease caused by a bacterium, *Candidatus Liberibacter asiaticus* (CLas), that has greatly affected citrus production in different parts of the world. Citrus trees get infected through CLas-infected Asian psyllid, an insect vector, which spreads the disease. This infection is followed by the appearance of visible symptoms, such as yellowing of the veins or of the entire leaf or botchy leaves, followed by deformed fruits, and eventual death of the tree (Chung and Brlansky, 2009). Although laboratory techniques such as polymerase chain reaction (PCR) provide accurate detection of HLB (Lacava et al., 2006; Li et al., 2009), efforts are being made on the development of field-based sensors (Hawkins et al., 2010; Sankaran et al., 2010, 2011) for rapid disease detection, which would control further spread of the disease. Presently, scouting for visible HLB symptoms is a common practice for identifying HLB-infected trees in the field. One of the major challenges during HLB detection during scouting is the differentiation of symptoms resulting from HLB and those due to nutrient deficiency. The similarity of these symptoms lowers the scouting efficiency and increases the need for better trained scouts, which is expensive and time-consuming. Therefore, there is a need for a handheld portable sensor that can potentially differentiate HLB symptoms from those caused by nutrient deficiency. In this study, we assess the applicability of fluorescence sensing for this purpose.

Recently, researchers have worked toward the rapid and early detection of abiotic and bioticstress in plants for precision agriculture applications. For example, some have investigated the use of laser-induced fluorescence spectroscopy for stress detection (mechanical stress, water stress, and citrus canker) in citrus under field and laboratory conditions (Marcassa et al., 2006; Belasque et al., 2008; Lins et al., 2009). Fluorescence sensing is one of the optical sensing techniques that is widely used for plant stress detection. Over the years, improved understanding of plant fluorescence has allowed researchers to apply fluorescence sensing towards plant health monitoring for several different crops (Van Kooten and Snel, 1990; Lichtenthaler et al., 1998; Bravo et al., 2004; Moshou et al., 2005; Lenk et al., 2007; Naumann et al., 2007; Chaerle et al., 2007a, 2007b; Belasque et al., 2008; Ehlert and Hincha, 2008).

Fluorescence emissions from plants can be broadly divided into two types. In the first type, emissions are from the leaf epidermis and fluorophores such as flavonoids, phenolics, NADH, and others, which are present in leaf veins. The major fluorescence output from natural or artificial UV excitation results from the leaf epidermis in the blue and green regions of the spectrum due to the presence of cinnamic acids such as ferulic acid (Lichtenthaler et al., 1998; Malenovský et al., 2009). The exciting light is interrupted by the epidermis to prevent photodegradation of internal leaf components. The second type of fluorescence emission occurs as a result of

Submitted for review in May 2011 as manuscript number IET 9205; approved for publication by the Information & Electrical Technologies Division of ASABE in January 2012.

The authors are **Sindhuja Sankaran, ASABE Member,** Post-Doctoral Research Associate, and **Reza Ehsani, ASABE Member,** Associate Professor, Department of Agricultural and Biological Engineering, Citrus Research and Education Center, IFAS, University of Florida, Lake Alfred, Florida. **Corresponding author:** Reza Ehsani, Department of Agricultural and Biological Engineering, Citrus Research and Education Center, IFAS, University of Florida, 700 Experiment Station Road, Lake Alfred, FL 33850; phone: 863-956-8771; fax: 863-956-4631; e-mail: ehsani@ufl.edu.

  ISSN 2151-0032

plant pigments such as chlorophyll. The chlorophyll absorbs the red and blue wavelengths; while carotenoids absorb photons from only the blue wavelength. The red and far-red (near-infrared) fluorescence is emitted by chlorophyll-*a* at room temperature (Cerovic et al., 1999; Malenovský et al., 2009). The first type fluorescence is broadly stated as "blue-green fluorescence," whereas the second type is specified as "chlorophyll fluorescence." The ratio of blue-green fluorescence to chlorophyll fluorescence depends on the plant type, exposure to sunlight, and proportion of fluorescence-absorbing materials present in the leaf. The chlorophyll excited with blue or red light yields a strong red and far-red fluorescence (Lichtenthaler et al., 1998). Nutrient deficiency in plants decreases the chlorophyll and carotenoid content, thereby decreasing their respective fluorescence emissions. Cerovic et al. (1999) described some of the specific fluorescence types and their contributing factors in detail.

In addition to the fluorescence, fluorescence ratios can also be used for monitoring physiological status of the plants. For example, the red to far-red fluorescence ratio decreases with increasing chlorophyll content in leaves (Buschmann, 2007; Malenovský et al., 2009). Similarly, the blue to red/far-red) fluorescence ratio with UV excitation is an indicator of physiological development, nutrition availability, and stress occurrence (Heisel et al., 1996; Malenovský et al., 2009). The other fluorescence ratios used for monitoring stress in citrus are the ratio of blue to red fluorescence, blue to far-red fluorescence, and red to far-red fluorescence (UV excitation) (Marcassa et al., 2006; Belasque et al., 2008; Lins et al., 2009). One of the challenges in fluorescence sensing is the high and varying light levels (Cerovic et al., 1999; Chaerle et al., 2007a). Thus, both laboratory and field evaluation is essential to account for the effect of environmental light variation.

This study evaluates a handheld multi-parameter fluorescence sensor for citrus plant stress (nutrient deficiency) and HLB disease detection. The findings reported in this study can help in the selection of critical fluorescence parameters related to nutrient deficiency and HLB infection.

Materials and Methods

Fluorescence Sensor

A Multiplex® 3 handheld multi-parameter optical sensor (Force-A, Orsay, France) is a real-time, non-destructive, active sensor that was used to collect fluorescence data from citrus leaves. This sensor (fig. 1) has been developed to evaluate the physiological status of plants using fluorescence sensing, with special emphasis on measuring fluorescence from chlorophyll, and constitutive and induced polyphenolics. It has been used in multiple applications (Tremblay et al., 2007; Cerovic et al., 2008; Zhang and Tremblay, 2010; Martinon et al., 2011). Numerous fluorescence outputs could be acquired from this instrument. Four excitation wavelengths were used: UV, blue (B), green (G), and red (R). For each of the excitation wavelengths, yellow (YF), red (RF), and far-red (near-infrared) (FRF) fluorescence were measured. Henceforth, the fluorescence output is labeled as: fluorescence output_excitation wavelength. For example, YF_UV represents yellow fluorescence with UV excitation. In addition to these 12 fluorescence features, fluorescence ratios were determined that include: (1) simple fluorescence ratio with green excitation (SFR_G), (2) simple fluorescence ratio with red excitation (SFR_R), (3) yellow to far-red fluorescence ratio with UV excitation (BRR_FRF), (4) fluorescence excitation ratio with red and UV excitation (FER_RUV), (5) fluorescence excitation ratio with red and green excitation (FER_RG), (6) flavonols (FLAV), (7) anthocyanins (ANTH), (8) nitrogen balance index with UV and green excitation (NBI_G), (9) nitrogen balance index with UV and red excitation (NBI_R), and (10) fluorescence excitation ratio anthocyanin relative index (FERARI).

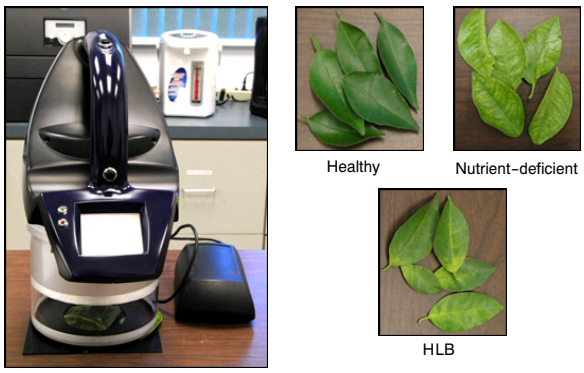

Figure 1. Handheld sensor unit and typical samples of citrus leaves used for acquiring fluorescence data.

The fluorescence sensor consists of LED-based units for providing excitation wavelengths and filtered photodiodes as detectors for measuring the fluorescence emissions from the canopy/leaf surface. The sensor has six UV (UV-A) and three RGB LED matrices. Similarly, the sensor has three synchronized photodiodes for detecting fluorescence emissions from the yellow, red, and far-red regions of the spectra (fig. 2). The sensor is capable of illumination at a distance of 10 cm from the light source (Martinon et al., 2011). An anodized aluminum black mask was used during data collection, which allowed fluorescence measurement in an area of about 191 cm^2 (7.8 cm dia.).

Data Collection

Fluorescence data were collected using a handheld fluorescence sensor during October 2010 from healthy, HLB-infected, and nutrient-deficient (zinc) citrus leaves (fig. 1). Thirty sample sets of each of the above categories from two sweet orange cultivars (Hamlin and Valencia) were analyzed. Each sample set of leaves consisted of four to five citrus leaves. Five replicate data were collected from each sample. Data were collected under field as well as controlled laboratory conditions. During field data collection, the handheld sensor was pointed toward the tree canopy, and measurements were acquired as illustrated in figure 2. Similarly, during laboratory data collection, the fluorescence data were collected by placing leaf samples (which were collected from the same tree canopy used for field data collection) on the table such that the leaves covered the entire region of the sensor sampling mask.

Before the data analysis, FERARI was eliminated. Moreover, the red to far-red fluorescence ratio (RFR_UV) (UV excitation) was computed by dividing RF_ UV by FRF_UV (Lichtenthaler et al., 1998; Cerovic et al., 1999; Belasque et al., 2008). It was observed that FRF_B and FRF_R values were saturated in the laboratory data. These values negative-

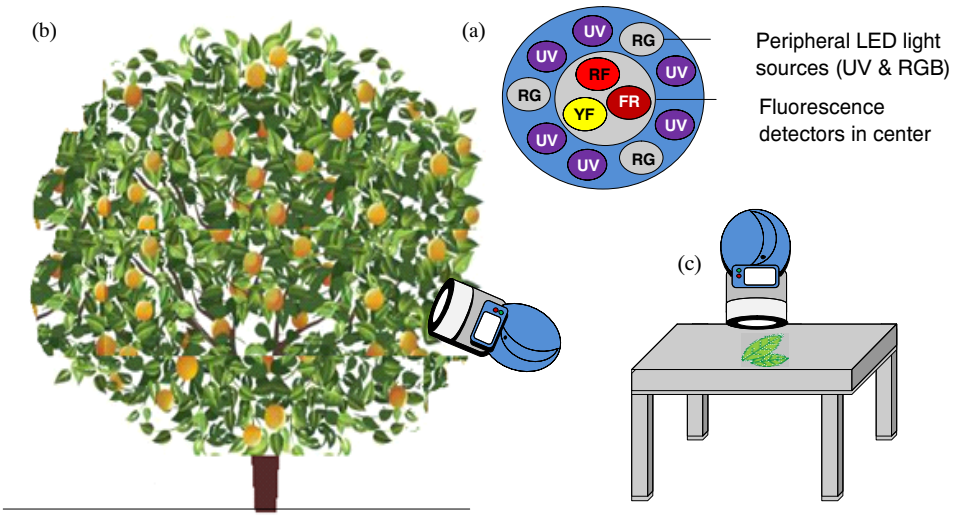

Figure 2. Sensor and data collection schematics: (a) arrangement of LED and detectors in the sensor, (b) field data collection procedure, and (c) laboratory data collection procedure.

ly affected the computation of SFR_R, FER_RUV, FLAV, FER_RG, ANTH, NBI_G, and NBI_R and therefore were not considered in the data analysis. Thus, the field dataset consisted of 22 fluorescence features, while the laboratory dataset consisted of 13 fluorescence features, as shown in table 1. The datasets and the total number of samples used for analysis are also described in table 1.

PCR Analysis

DNA was extracted from the leaf samples using the Wizard Genomic DNA purification kit (Promega Corp., Madison, Wisc.) by following the protocol for isolating genomic DNA from plant tissue. PCR using primers A2 and JS was performed to confirm the presence of CLas in the samples (Hocquellet et al., 1999). Amplification of DNA was determined by electrophoresis on 1.2% agarose gels for 30 to 45 min and visualized by ethidium bromide staining. The 703-bp amplicon from the 16s rRNA gene is indicative of the presence of CLas. Sample PCR gel electrophoresis results are shown in figure 3. PCR results revealed that two of the HLB-infected samples of the Hamlin cultivar were PCR negative. Therefore, the fluorescence data of these two samples were removed from the dataset.

Data Analysis

Classification of the fluorescence features was performed using the Naïve-Bayes and the bagged decision tree classifiers. The Naïve-Bayes (Ivanov et al., 2002; Huang et al., 2007; Pant et al., 2010) is a simple classifier, with the capability of effective supervised learning though probability analysis. It estimates the probability or probability density of features for a given class. If Y is considered to be the class label and X_1 to X_i indicate the variables (fluorescence features), then the probability of Y given X_1 to X_i according to the Naïve-Bayes model is:

$$p(Y \mid X_1, X_2, \ldots X_i) = p(Y \mid X) = \frac{p(Y)\, p(X_1, X_2, \ldots X_i \mid Y)}{p(X_1, X_2, \ldots X_i)} \quad (1)$$

$$p(Y \mid X) = \frac{p(Y) p(X \mid Y)}{p(X)} \quad (2)$$

The $p(X|Y)$ and $p(Y)$ are estimated based on the $p(Y|X)$ during the model training, i.e., Bayes estimation. In the testing phase (test dataset), $p(Y|X)$ is determined using the $p(X|Y)$ and $p(Y)$ estimates from the training dataset (Mitchell, 1997).

A kernel smoothing density estimate was used during the implementation of the Naïve-Bayes model as it did not require a strong assumption of normal distribution. During the classification, a normal kernel density estimate was computed for each class based on the training data for that particular class. Assuming that the data followed a Gaussian distribution, the kernel density estimation will eliminate skewness and multiple peaks. One of the basic assumptions of this model is that the features are independent within each class. In this study, few fluorescence features showed high correlation. For example, in all datasets, RF_UV and FRF_UV, RF_G and FRF_G, and RF_B and RF_G were highly correlated. It was anticipated that the classifier would perform well even if the assumption of correlation is not valid.

The bagged decision tree (classification tree) classifier is a type of supervised ensemble learning algorithm with higher stability and improved performance (Khan et al., 2001; Huang et al., 2004) compared to decision trees. The tree bagger is an ensemble of decision trees (Breiman et al., 1984). If the response variable Y is a function of predictor variables

Table 1. Fluorescence datasets used for analysis.

Dataset	Cultivar	Field or Lab	No. of Samples	No. of Features
Hamlin-Field	Hamlin	Field	440[a]	22
Hamlin-Lab	Hamlin	Lab	440[a]	13
Valencia-Field	Valencia	Field	450	22
Valencia-Lab	Valencia	Lab	450	13
Combined-Field	Hamlin+Valencia	Field	890	22
Combined-Lab	Hamlin+Valencia	Lab	890	13

[a] In general, the number of samples was: 30 sample sets × 3 categories × 5 replicates = 450. Two samples of the HLB-infected category for Hamlin were PCR negative; therefore, their fluorescence features were removed before data analysis.

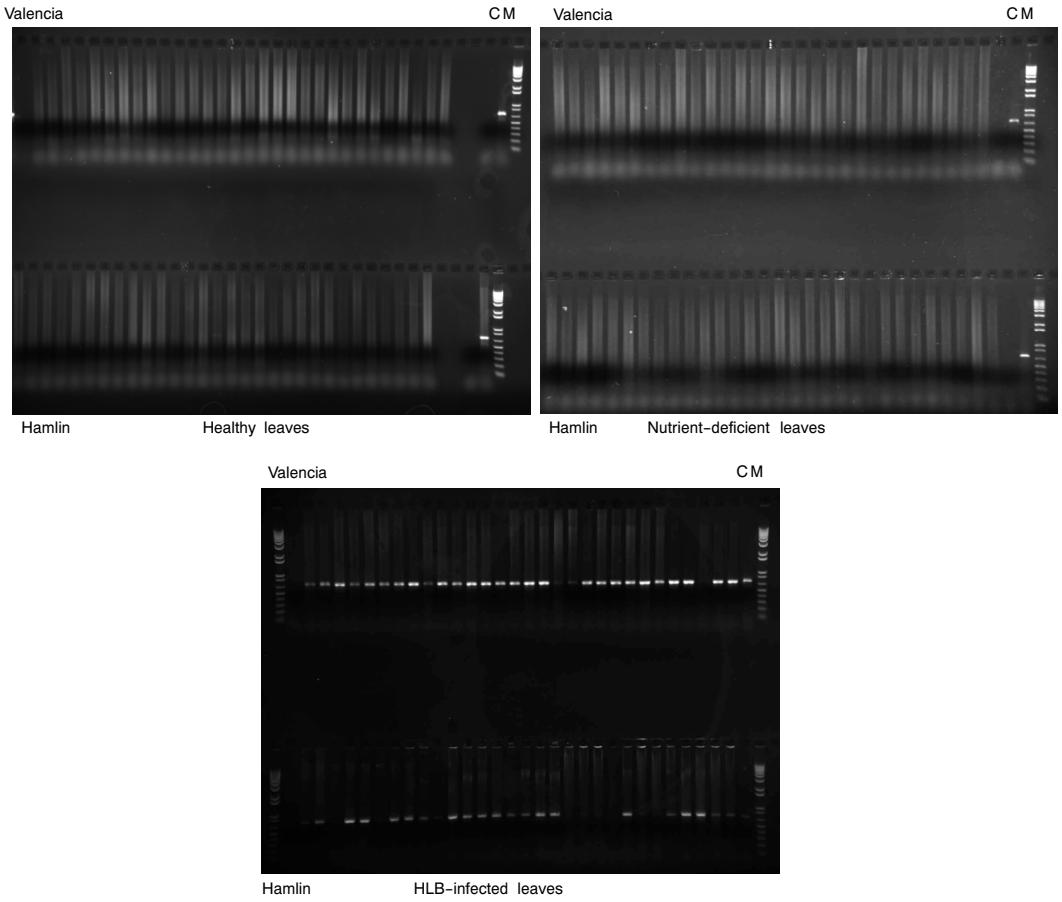

Figure 3. Conventional polymerase chain reaction analysis results for the detection of *Candidatus Liberibacter asiaticus* in three categories of citrus leaves investigated in this study (lane M = DNA molecular weight markers; lane C = positive control).

X_1 to X_i (fluorescence features) in the classification tree, a binary tree/subset is generated with a branching node based on the information provided by predictor variables. These subsets or nodes are termed terminal nodes (two classes in this case).

$$Y = f(X_1, X_2, \ldots X_i) \quad (3)$$

The classification tree is developed using the predictor (X) and response (Y) variables of the training dataset. The class (Y) of an unknown sample in the test dataset is then predicted based on the set of splitting rules conceived during the training. In this study, Gini's diversity index algorithm was used for estimating the splitting rules. The bagging generates bootstrap replicates to strengthen the decision tree. It also improves the unbiased base learning of the model (decision trees). During bagging (bootstrap aggregation), every classification tree is grown on an independently drawn bootstrap replica of the input data. In this study, 150 decision trees based on bootstrap replicas were used to generate the ensemble decision tree. This number was optimized during preliminary studies. Although the bagged decision tree classifier offers higher flexibility, the Naïve-Bayes classifier is simpler and faster. In order to improve the speed and performance of the classifiers, sequential feature selection (forward selection) was used. This feature selection method minimizes the number of features based on the lowest possible misclassification rate for the classifier. In sequential forward selection, from an empty set, each feature is added sequentially until there is no further improvement in classification accuracy using a specific classifier. The performance of the classifiers with and without feature selection was evaluated.

A Matlab program (ver. 7.11, The MathWorks, Inc., Natick, Mass.) was used for the data analysis. For implementing the classification and feature selection, Statistics Toolbox 7 was used. A Hewlett-Packard EliteBook 8740w computer, with a processor speed of 2.13 GHz and 8 GB of internal memory was used to run the Matlab program. The fluorescence datasets (table 1) were randomized and divided into training and testing datasets such that their ratio was 3:1. Classifier performance was assessed based on cross-validation classification error, classification error, and the computation time for classifying fluorescence values of HLB-infected leaves from those of nutrient-deficient and healthy leaves. The classifier parameters were estimated for multiple datasets possessing variation in data collection condition (field, laboratory), type (Hamlin, Valencia, Hamlin and Valencia combined), and analysis (with and without feature extraction) for both classifiers. To determine the cross-validation error, a 10-fold stratified cross-validation was performed with the training dataset.

Results and Discussion

Classification

Table 2 presents the cross-validation and classification results of the Naïve-Bayes and bagged decision tree classifiers. Comparing the field and laboratory datasets, the cross-

Table 2. Validation and classification results of Naïve-Bayes and bagged decision tree classifiers with and without feature extraction.[a]

	Naïve-Bayes Classifier						Bagged Decision Tree Classifier					
	CVE	CE	CT (s)	Fluorescence Features	CE[b]	CT[b] (s)	CVE	CE	CT (s)	Fluorescence Features	CE[b]	CT[b] (s)
Field dataset												
Hamlin	0.17	0.17	1.5	YF_UV, RF_B, FRF_B, SFR_G, FLAV	0.05	0.2	0.05	0.05	21.2	YF_UV, FRF_B, FRF_R, SFR_G, SFR_R, FER_RUV, NBI_R	0.07	6.3
Valencia	0.29	0.22	1.2	YF_UV, BRR_FRF, FER_RG, NBI_G, NBI_R	0.18	0.2	0.06	0.04	25.1	YF_UV, RF_B, YF_R, SFR_R, BRR_FRF, ANTH, NBI_R	0.04	7.6
Combined	0.28	0.32	2.0	YF_UV, FRF_B, SFR_G, FER_RG, NBI_R	0.22	0.3	0.07	0.05	26.5	YF_UV, RF_UV, YF_G, FRF_G, YF_R, SFR_G, ANTH, NBI_R, RFR_UV	0.06	10.6
Laboratory dataset												
Hamlin	0.11	0.11	0.5	YF_UV, RF_UV, YF_G	0.06	0.1	0.01	0.02	6.6	YF_UV, FRF_UV, YF_G, SFR_G, BRR_FRF	0.02	5.0
Valencia	0.14	0.14	1.0	YF_UV, FRF_UV, RF_B, YF_G, FRF_G, BRR_FRF, RFR_UV	0.07	0.2	0.04	0.04	9.4	YF_UV, YF_G, FRF_G	0.02	4.6
Combined	0.17	0.10	0.7	YF_UV, FRF_UV, YF_G, FRF_G, BRR_FRF, RFR_UV	0.07	0.3	0.04	0.04	11.2	YF_UV, RF_UV, FRF_UV, RF_B, YF_G, SFR_G	0.04	8.5

[a] CVE = cross-validation classification error, CE = classification error, CT = computation time.
[b] After the fluorescence feature extraction process.

Table 3. Overall and individual class classification accuracies (%) of Naïve-Bayes and bagged decision tree classifiers with and without feature extraction.

	Field Dataset			Laboratory Dataset		
Classifier	Hamlin	Valencia	Combined	Hamlin	Valencia	Combined
Naïve-Bayes classifier without feature extraction						
Overall	82.7	77.7	68.3	89.1	85.7	90.1
Healthy	94.7	78.9	80.0	89.5	97.4	94.7
Nutrient-deficient	70.3	75.7	56.0	89.2	64.9	82.7
HLB-infected	82.9	78.4	69.0	88.6	94.6	93.1
Naïve-Bayes classifier with feature extraction						
Overall	95.5	82.1	77.9	93.6	92.9	92.8
Healthy	100.0	84.2	89.3	89.5	97.4	98.7
Nutrient-deficient	100.0	81.1	69.3	91.9	81.1	81.3
HLB-infected	85.7	81.1	75.0	100.0	100.0	98.6
Bagged decision tree classifier without feature extraction						
Overall	94.5	96.4	94.6	98.2	96.4	96.4
Healthy	97.4	94.7	96.0	94.7	100.0	98.7
Nutrient-deficient	94.6	97.3	92.0	100.0	91.9	90.7
HLB-infected	91.4	97.3	95.8	100.0	97.3	100.0
Bagged decision tree classifier with feature extraction						
Overall	92.7	96.4	94.1	98.2	98.2	96.4
Healthy	94.7	94.7	94.7	94.7	100.0	97.4
Nutrient-deficient	94.6	97.3	92.0	100.0	97.3	92.0
HLB-infected	88.6	97.3	95.8	100.0	97.3	100.0

validation error and classification error were lower in the laboratory dataset for Hamlin and Valencia, using both the classifiers, than in the corresponding field dataset. This trend was expected, as the laboratory dataset would possess lower variability in the fluorescence values due to the controlled data collection conditions. The cross-validation and classification errors for the Naïve-Bayes classifier varied from 0.17 to 0.29 and from 0.17 to 0.32, respectively, for the field dataset. However, the corresponding errors for the laboratory dataset were 0.11 to 0.17 and 0.10 to 0.14. It was observed that, unlike the reduction in classification error from field to laboratory datasets for the Naïve-Bayes classifier, the bagged decision tree classifier did not exhibit significant reduction in the classification error. Thus, it could be stated that the bagged decision tree classifier worked well for the classification of both field and laboratory datasets. In addition, when the two classifiers were compared, the bagged decision tree classifier performed better than the Naïve-Bayes classifier in terms of lower cross-validation and classification errors.However, the computation time of the Naïve-Bayes classifier was lower, taking less than 2 s in most cases to compute the classification accuracies. In the Naïve-Bayes classifier, the construction of the classification algorithm is much faster than in the bagged decision tree classifier. We found that the Naïve-Bayes classifier was at least 10 times faster.

The overall and individual class classification accuracies were computed using the confusion matrix is presented in table 3. The overall classification accuracy of the Naïve-Bayes classifier for the field and laboratory datasets varied from 68% to 83% and from 86% to 90%, respectively. The HLB-class classification accuracy under laboratory conditions was slightly higher than those of field conditions, especially for the Hamlin cultivar. The classification accuracy increased by 7% and higher under laboratory conditions. Comparing the HLB-class classification accuracy, the Naïve-Bayes classifier showed accuracy of greater than 88% under laboratory conditions for both citrus cultivars. Thus, if the fluorescence sensor were to be used for detecting HLB with the Naïve-Bayes classifier, then faster and more accurate results could be acquired by removing the citrus leaves from the canopy, placing them on a flat surface, and collecting data under stable conditions. The bagged decision tree classifier showed an overall and HLB-class classification accuracy greater than 94% and 91%, respectively. Therefore, the bagged decision tree classifier with the fluorescence sensor might be more applicable in remotely detecting HLB in a tree canopy under field conditions.

Feature Extraction

Feature extraction using forward sequential selection was performed to identify significant fluorescence features that can contribute to the classification of fluorescence data for each dataset. The fluorescence features and classifier performance in terms of classification accuracy and computation time are reported in tables 2 and 3. The feature selection process reduced the computation time and improved the overall and HLB-class classification accuracies by 3% and higher, especially for the Naïve-Bayes classifier. Thus, with selected features, under controlled conditions, the Naïve-Bayes classifier with fluorescence sensor can be used for more accurate HLB detection.

Different fluorescence features can contribute or represent different classes under each condition. For example, Malenovský et al. (2009) reported that the red to far-red fluorescence ratios decrease with increasing chlorophyll content. From figures 4 and 5, it can be observed that the red to far-red fluorescence values were lower in healthy leaves than in nutrient-deficient and HLB-infected leaves for both Hamlin and Valencia cultivars. This might be due to higher chlorophyll content in the healthy leaves than in the stressed leaves. Using the feature extraction method, it was observed that yellow fluorescence with UV excitation always contributed to the classification of healthy, nutrient-deficient, and

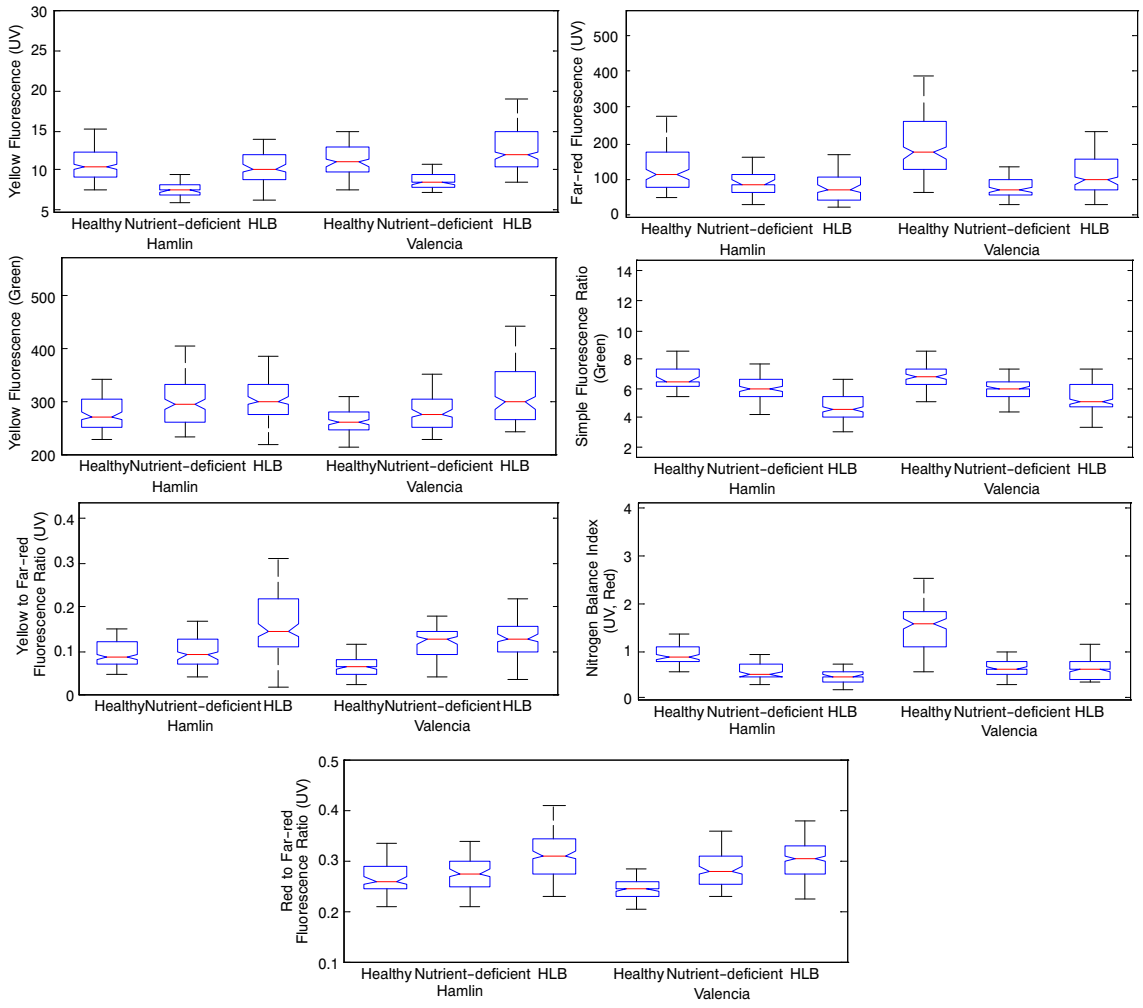

Figure 4. Selected fluorescence features of the field dataset.

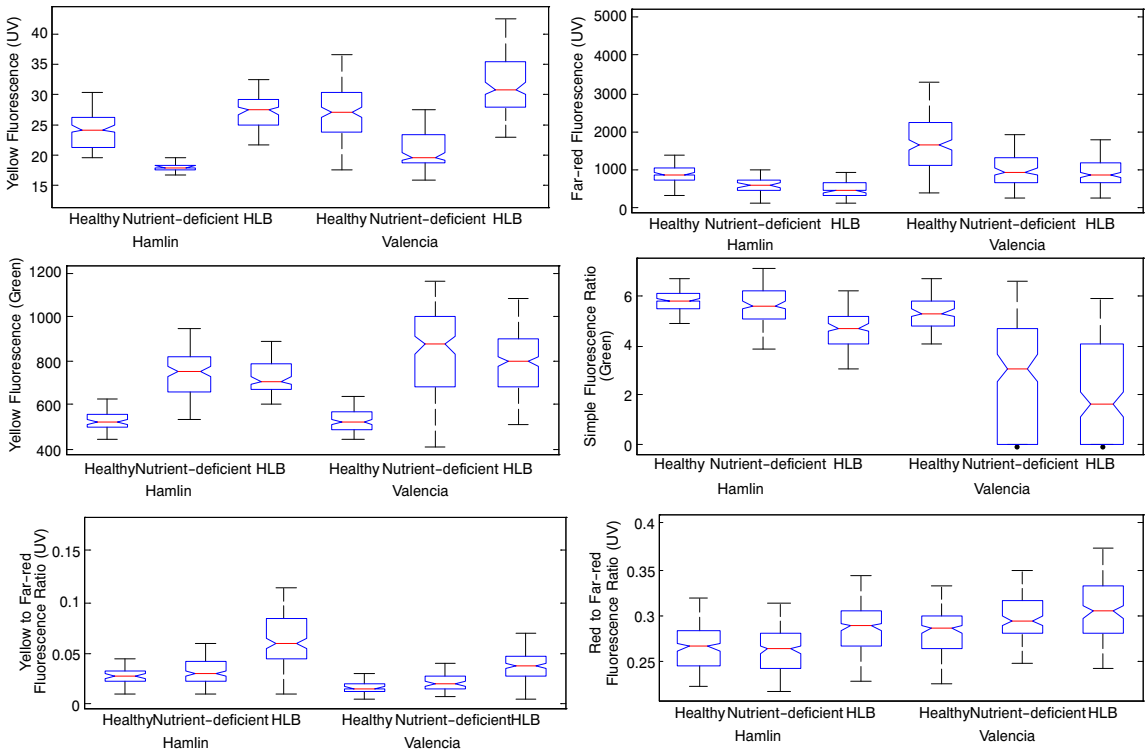

Figure 5. Selected fluorescence features of the laboratory dataset.

HLB-infected leaves. Some of the other features were far-red fluorescence (UV), yellow fluorescence (green), simple fluorescence ratio (green), yellow to far-red fluorescence ratio (UV), and nitrogen balance index (UV, red). The yellow fluorescence (green) and far-red fluorescence (UV) were important fluorescence features under laboratory conditions, while nitrogen balance index (UV, red) was the prominent feature for field conditions.

Among the different excitations, UV-induced fluorescence has been extensively used in remote sensing applications for stress detection due to its sensitivity. Cerovic et al. (1999) reported that UV-excited fluorescence is a good indicator to accurately evaluate the physiological status of plants and detect stress. A similar trend can be observed in this study. Comparing the different fluorescence features, it could be observed that the UV-excited fluorescence features are more prominent for classifying healthy and stressed leaves (nutrient-deficient, HLB) than the other fluorescence features. The red and far-red fluorescence with UV excitation could be a major contributor to the chlorophyll-*a* present in the leaves (Cerovic et al., 1999). Both red and far-red fluorescence (UV) values were found to be higher in healthy leaves than in nutrient-deficient and HLB-infected leaves. Therefore, this study demonstrates the applicability of using fluorescence sensing for HLB-detection in citrus.

Summary

This study demonstrates the potential of using handheld fluorescence sensing for stress detection in citrus leaves, especially HLB detection in citrus. Both the Naïve-Bayes and bagged decision tree models resulted in higher classification accuracies under laboratory (controlled) conditions than field conditions. Comparing the classifiers, the bagged decision tree classifier yielded higher classification accuracy, although the computation time was at least 10 times greater than that of the Naïve-Bayes classifier. Fluorescence feature extraction improved the classification accuracy under both laboratory and field conditions, especially for the Naïve-Bayes classifier. Among the fluorescence features and ratios acquired from the portable fluorescence sensor, it was found that yellow fluorescence (UV) and simple fluorescence ratio (green) contributed to the classification of leaf conditions. Moreover, yellow fluorescence (green) and far-red fluorescence (UV) contributed to the classification of leaves under controlled conditions, while nitrogen balance index (red) contributed to the classification under field conditions.

Research indicates that other fluorescence features such as blue fluorescence (UV) and related ratios can also be a good indicator of the physiological status of plants. Our future studies will involve the evaluation of these fluorescence features as well as other ratios for HLB detection in citrus. In addition, we intend to collect a larger dataset of fluorescence features from multiple citrus cultivars to further improve the classification accuracies.

Acknowledgements

We would like to thank the Citrus Research and Development Foundation (CRDF) and the USDA National Institute of Food and Agriculture (NIFA) for their funding for this research. We would also like to extend our special thanks to Ms. Luba Polonik, Ms. Cindy Basnaw, Ms. Lin Yang, Dr. Aswathy Sreedharan, Ms. Sherrie Buchanon, Dr. Pankaj Trivedi, and Dr. Nian Wang for their help during the study.

REFERENCES

Belasque, L., M. C. G. Gasparoto, and L. G. Marcassa. 2008. Detection of mechanical and disease stresses in citrus plants by fluorescence spectroscopy. *Applied Optics* 47(11): 1922-1926.

Bravo, C., D. Moshou, R. Oberti, J. West, A. McCartney, L. Bodria, and H. Ramon. 2004. Foliar disease detection in the field using optical sensor fusion. *Agric. Eng. Intl.: CIGR E-Journal* 6: Manuscript FP 04 008.

Breiman, L., J. Friedman, R. Olshen, and C. Stone. 1984. *Classification and Regression Trees.* Boca Raton, Fla.: CRC Press.

Buschmann, C. 2007. Variability and application of the chlorophyll fluorescence emission ratio red/far-red of leaves. *Photosynthesis Research* 92(2): 261-271.

Cerovic, Z. G., G. Samson, F. Morales, N. Tremblay, and I. Moya. 1999. Ultraviolet-induced fluorescence for plant monitoring: Present state and prospects. *Agronomie* 19(7): 543-578.

Cerovic, Z. G., N. Moise, G. Agati, G. Latouche, N. Ben Ghozlen, and S. Meyer. 2008. New portable optical sensors for the assessment of winegrape phenolic maturity based on berry fluorescence. *J. Food Comp. and Analysis* 21(8): 650-654.

Chaerle, L., I. Leinonen, H. G. Jones, and D. Van Der Straeten. 2007a. Monitoring and screening plant populations with combined thermal and chlorophyll fluorescence imaging. *J. Exp. Botany* 58(4): 773-784.

Chaerle, L., S. Lenk, D. Hagenbeek, C. Buschmann, and D. Van Der Straeten. 2007b. Multicolor fluorescence imaging for early detection of the hypersensitive reaction to tobacco mosaic virus. *J. Plant Physiol.* 164(3): 253-262.

Chung, K. R., and R. H. Brlansky. 2009. Citrus diseases exotic to Florida: Huanglongbing (citrus greening). Fact sheet PP-210. Gainesville, Fla.: University of Florida IFAS, Florida Cooperative Extension Service.

Ehlert, B., and D. K. Hincha. 2008. Chlorophyll fluorescence imaging accurately quantifies freezing damage and cold acclimation responses in Arabidopsis leaves. *Plant Methods* 4: Article 12.

Hawkins, S. A., B. Park, G. H. Poole, T. Gottwald, W. R. Windham, and K. C. Lawrence. 2010. Detection of citrus Huanglongbing by Fourier transform infrared-attenuated total reflection spectroscopy. *Applied Spectroscopy* 64(1): 100-103.

Heisel, F., M. Sowinska, J. A. Miehe, M. Lang, and H. K. Lichtenthaler. 1996. Detection of nutrient deficiencies of maize by laser-induced fluorescence imaging. *J. Plant Physiol.* 148(5): 622-631.

Hocquellet, A., P. Toorawa, J. M. Bové, and M. Garnier. 1999. Detection and identification of the two *Candidatus Liberobacter* species associated with citrus Huanglongbing by PCR amplification of ribosomal protein genes of the β operon. *Molecular and Cellular Probes* 13(5): 373-379.

Huang, Y., J. Cai, L. Ji, and Y. Li. 2004. Classifying G-protein coupled receptors with bagging classification tree. *Computational Biol. and Chem.* 28(4): 275-280.

Huang, Y., P. McCullagh, N. Black, and R. Harper. 2007. Feature selection and classification model construction on type 2 diabetic patients' data. *Artificial Intelligence in Med.* 41(3): 251-262.

Ivanov, O., M. M. Wagner, W. W. Chapman, and R. T. Olszawski. 2002. Accuracy of three classifiers of acute gastrointestinal syndrome for syndromic surveillance. In *Proc. AMIA 2002 Annual Symp. Proc*., 345-349. Bethesda, Md.: American Medical Informatics Association.

Khan , J., J. S. Wei, M. Ringnér, L. H. Saal, M. Ladanyi, F. Westermann, F. Berthold, M. Schwab, C. R. Antonescu, C. Peterson, and P. S. Meltzer. 2001. Classification and diagnostic prediction of cancers using gene expression profiling and artificial neural networks. *Nature Med.* 7(6): 673-679.

Lacava, P. T., W. B. Li, W. L. Araújo, J. L. Azevedo, and J. S. Hartung. 2006. Rapid, specific, and quantitative assays for the detection of the endophytic bacterium *Methylobacterium mesophilicum* in plants. *J. Microbiol. Methods* 65(3): 535-541.

Lenk, S., L. Chaerle, E. E. Pfündel, G. Langsdorf, D. Hagenbook, H. K. Lichtenthaler, D. Van Der Straeten, and C. Buschhmann. 2007. Multispectral fluorescence and reflectance imaging at the leaf level and its possible applications. *J. Exp. Botany* 58(4): 807-814.

Li, W., J. A. Abad, R. D. French-Monar, J. Rascoe, A. Wen, N. C. Gudmestad, G. A. Secor, I. M. Lee, Y. Duan, and L. Levy. 2009. Multiplex real-time PCR for detection, identification, and quantification of '*Candidatus Liberibacter solanacearum*' in potato plants with zebra chip. *J. Microbiol. Methods* 78(1): 59-65.

Lichtenthaler, H. K., O. Wenzel, C. Buschmann, and A. Gitelson. 1998. Plant stress detection by reflectance and fluorescence. *Annals New York Acad. Sci.* 851(1): 271-285.

Lins, E. C., J. Belasque Jr., and L. G. Marcassa. 2009. Detection of citrus canker in citrus plants using laser-induced fluorescence spectroscopy. *Precision Agric.* 10(4): 319-330.

Malenovský, Z., K. B. Mishra, F. Zemek, U. Rascher, and L. Nedbal. 2009. Scientific and technical challenges in remote sensing of plant canopy reflectance and fluorescence. *J. Exp. Botany* 60(11): 2987-3004.

Marcassa, L. G., M. C. G. Gasparoto, J. Belasque Jr., E. C. Lins, F. Dias Nunes, and V. S. Bagnato. 2006. Fluorescence spectroscopy applied to orange trees. *Laser Physics* 16(5): 884-888.

Martinon, V., E. M. Fadailli, S. Evain, and C. Zecha. 2011. Multiplex: An innovative optical sensor for diagnosis, mapping, and management of nitrogen on wheat. In *Proc. 8th European Conf. on Precision Agriculture*. Prague, Czech Republic: Czech Center for Science and Society.

Mitchell, T. M. 1997. *Machine Learning.* New York, N.Y.: McGraw-Hill.

Moshou, D., C. Bravo, R. Oberti, J. West, L. Bodria, A. McCartney, and H. Ramon. 2005. Plant disease detection based on data fusion of hyperspectral and multispectral fluorescence imaging using Kohonen maps. *Real-Time Imaging* 11(2): 75-83.

Naumann, J. C., D. R. Young, and J. E. Anderson. 2007. Linking leaf chlorophyll fluorescence properties to physiological responses for detection of salt and drought stress in coastal plant species. *Physiologia Plantarum* 131(3): 422-433.

Pant, B., K. Pant, and K. R. Pardasani. 2010. Naïve-Bayes classifier for classification of plant and animal miRNA. *Intl. J. Computer Theory and Eng.* 2(3): 1793-8201.

Sankaran, S., A. Mishra, R. Ehsani, and C. Davis. 2010. A review of advanced techniques for detecting plant diseases. *Computers and Electronics in Agric.* 72(1): 1-13.

Sankaran, S., A. Mishra, J. M. Maja, and R. Ehsani. 2011. Visible/near-infrared spectroscopy for detection of Huanglongbing in citrus orchards. *Computers and Electronics in Agric.* 77(2): 127-134.

Tremblay N., Z. Wang, and C. Belec. 2007. Evaluation of the Dualex for the assessment of corn nitrogen status. *J. Plant Nutrition* 30(7-9): 1355-1369.

Van Kooten, O., and J. F. H. Snel. 1990. The use of chlorophyll fluorescence nomenclature in plant stress physiology. *Photosynthesis Research* 25(3): 147-150.

Zhang, Y. P., and N. Tremblay. 2010. Evaluation of the Multiplex fluorescence sensor for the assessment of corn nitrogen status. In *Proc. 10th Intl. Conf. on Precision Agriculture.* International Society of Precision Agriculture.